Development and Workspace Study of a 4-PP Planar Parallel XY Positioning Stage Using SMA Actuators

Rutupurna Choudhury, Deep Singh, Anuj Kumar, Yogesh Singh, and Chinmaya Kumar Sahoo

Abstract The necessity to fabricate micron-sized objects at present is increasing rapidly. Planar parallel manipulators, an area of robotics, is also employed to develop motion stages for various applications. The present study proposes a 4-PP planar positioning motion stage. The end-effector of the proposed positioning stage undergoes motion along both the axis in a plane and restricts any angular motion. The planar parallel positioning device (manipulator) possesses four active input prismatic joints which are actuated by implementing Shape Memory Alloy (SMA) based smart material springs. The SMA spring-based actuators are very lightweight and provide higher work per unit mass in comparison to other actuators. The proposed manipulator possesses two degrees of freedom. This study presents the workspace analysis of the proposed manipulator actuated by smart materials. The study depicts the experimental workspace efficiency of 42.87% for the proposed motion stage in comparison to the feasible workspace region. The planar parallel motion stage has the ability to displace in microns within the workspace domain. This study also shows the adequacy of SMA spring-based actuators in the development of micro-positioning devices.

Note: P represents a prismatic joint.

Keywords Positioning stage · Planar parallel manipulator · Shape memory alloy

R. Choudhury · D. Singh · A. Kumar · Y. Singh (✉) · C. K. Sahoo
Mechanical Engineering, National Institute of Technology Silchar, Silchar, Assam 788010, India
e-mail: yogeshsingh15@gmail.com

R. Choudhury
e-mail: rutupurna.choudhury10@gmail.com

D. Singh
e-mail: deepsingh.0318@gmail.com

A. Kumar
e-mail: anujpal096@gmail.com

C. K. Sahoo
e-mail: chinmaya.cks@gmail.com

1 Introduction

Automation is one of the important parts of any industry. Nowadays, necessity of automation is vital in every field like industry, medical, transportation, etc. Robotics is one of the keys to automation. It plays a vital role in automating manual activities. Planar parallel manipulators (PPM) is an important content to robotics. An *XY* positioning stage is a PPM device used for movement and positioning of object. The *XY* positioning mechanism is driven by actuators for its motion and possesses wide applications including material handling and processing, micro-machining, fabrication, etc. *XY* motion stage is also used for precise positioning of objects or components. The literature consists of various planar positioning devices that actuate on conventional motors which are bulky and requires higher current as driving force. Presently, smart materials like shape memory alloy (SMA), piezoelectric material, etc., have gained remarkable recognition due to their great potential and self-transformation properties [1]. Fesperman et al. [2] developed an *XY* stage driven by linear motor which floats on a thin film of air. The object was displaced using three heterodyne displacement sensors. The object has the ability to displace 10 mm along both *X*- and *Y*-axes. The overall size of the position stage mechanism was 477 m^2. Shimizu et al. [3] developed millimetre-order *XY* micro-motion stage to position lightweight objects precisely. This positioning stage is driven by friction to recognize long range travel motion with the help of small stroke piezoelectric actuators. Lee et al. [4] designed a novel micro-*XY* motion stage mechanism with the application of thermal actuators. This motion was carried out by the thermal expansion force of the SU-8 thermal actuators. This actuator has the maximum displacement of 41 μm at 250 °C. This material is more suitable for an actuator that needs large displacement for use in micro-*XY* stages. Basic design issues like static, dynamic and tracking control are investigated by Qin et al. [5]. It addresses the fundamental problems of establishing a decoupled *XY* stage motion mechanism. The motion is carried out by two piezoelectric actuators. It was observed that the statically indeterminate structures are able to decouple the cross-axis coupling with increased stiffness and stability. Yao et al. [6] studied the design and the performance of parallel micro-positioning *XY* motion stage mechanism. This is also driven by piezoelectric actuators. The kinematic and dynamic study showed that the stage possesses larger workspace, good linearity and high bandwidth as compared to the serial kinematic designs. Wang et al. [7] studied the design of the flexure-based *XY* precision stage and obtained large task space under reduced driving force. Choi et al. [8] developed an *XY* stage motion mechanism by considering cross-strip flexure joints and over-constrained mechanism. The motion stage is composed of flexural joints, links and is driven by a linear motor. For large rotation cross-strip, flexural joints are used. Horizontal straightness, repeatability test and yaw are studied in this work. From the literature, it was observed that SMA actuators can be used as the best substitute for conventional actuators like servomotors, hydraulics and pneumatics [9] because of its unique behaviour and mechanical properties. So, this leads to the development of advanced and cost-effective actuators with a considerable reduction in complexity, weight and size. Chang-Jun et al. [10]

developed a micro-wheeled robotic device using SMA actuator. Similarly, Kim et al. [11] developed an earthworm-based micro-robot using SMA spring as actuator.

1.1 Contribution in the Present Paper

This paper presents the SMA spring actuation-based 4-PP XY micro-motion stage mechanism and addresses the development of conceptual design and kinematics of the manipulator. In addition, feasible workspace analysis is also presented. The proposed motion stage consists of two legs configured prismatic-prismatic along *X*-direction and the other two legs configured prismatic-prismatic along *Y*-direction. The motion stage consists of four active prismatic joints at each leg actuated by nitinol (NiTi) SMA springs. The 4-PP *XY* micro-motion stage was fabricated, and the experiment was performed to determine the associated workspace and also the feasibility of smart materials for the development of the motion stage. The manipulator is designed in such a way that the angular orientation of the end-effector is restricted.

2 Shape Memory Alloy Actuator

Smart materials have the potential to recover large strains due to transformation in phase from martensite (lower temperature) to austenite (higher temperature) as in case of SMAs [12]. SMA or nitinol spring possesses a special behaviour called shape memory effect (SME) [9, 12]. This exceptional characteristic is the prime reason behind the wide application of the SMA in different fields like the surgical tool, aeronautical application and micro-actuators. According to the microscopic studies, SMA rearranges its crystal structure during phase transformation under the application of heat. This is the mechanism of SMA to recover its original shape. The major advantage of SMA is that it could restore its original memorized shape under thermal loading [9]. The SMA implemented as an actuator in the present study is nitinol tension spring of 0.75 mm wire diameter. It can elongate and contract maximum up to 140 mm and 29 mm, respectively. The material has Young's modulus and density of 120 MPa and 6.4 E-06 kg/mm^3, respectively.

3 Development of Smart Actuation-Based XY Micro-motion Stage

This paper presents the SMA actuation based XY micro-motion stage. The paper studies the workspace associated with the XY motion stage by implementing smart
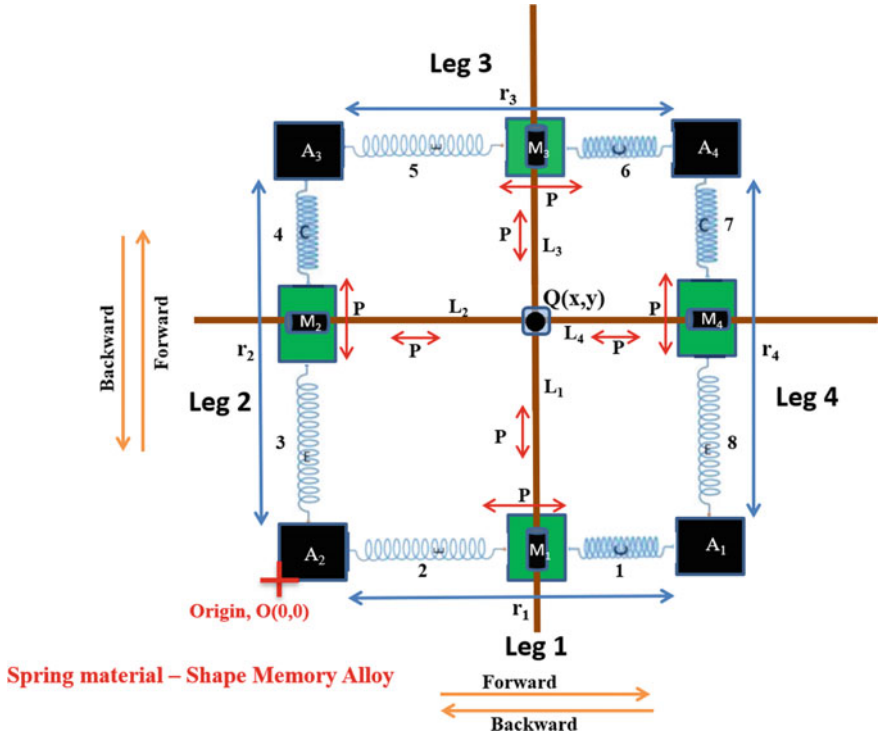
Fig. 1 Schematic diagram of SMA spring actuation-based 4-PP *XY* motion stage mechanism

material, nitinol spring, as actuators for the active prismatic joints as depicted in Fig. 1.

Figure 1 illustrates the schematic diagram of shape memory alloy spring actuation-based *XY* robotic micro-motion stage. The *XY* motion stage consists of four legs of which each leg has prismatic-prismatic (PP) configuration. All the four legs of equal lengths together form a square configuration as depicted in Fig. 1. This device consists of eight numbers of nitinol SMA springs $(1 - 8)$ as actuators for the active input prismatic joints $(M_1, M_2, M_3$ and $M_4)$. Each leg consists of two springs at either side of the active prismatic joints which help to undergo bidirectional movement along its orientation axis. The contraction of the springs $(1, 6)$ and $(2, 5)$ results in forward and backward motion of the end-effector along *X*-axis, respectively. Similarly, the contraction of the springs $(4, 7)$ and $(3, 8)$ results in forward and backward motion of the end-effector along *Y*-axis, respectively. The blocks A_1, A_2, A_3 and A_4 are fixed to which one end of the SMA springs is connected forms the fixed base. The other ends of the SMA springs are connected to the active prismatic joints $(M_1, M_2, M_3$ and $M_4)$. The links L_1 and L_2 form passive prismatic joints at M_1, M_2, M_3 and M_4 of each leg. The links L_1 and L_2 form a rigid joint at a point (Q) which is known as the end-effector of the motion platform. The r_1, r_2, r_3 and r_4 at each leg represent the stroke

length of the active input translational joints which is directly proportional to the amount of contraction of either spring at the respective legs. The coordinates or the pose of the end-effector is represented as (Q_x, Q_y). The manipulator does not possess any revolute joints in order to avoid the rotation of the end-effector. Further, to avoid the end-effector rotation, the active prismatic joints (r_1 and r_3) and (r_2 and r_4) are actuated simultaneously and maintained the same value. 'C' and 'E' represented on the springs indicate its deformed nature as compressed and elongated, respectively.

3.1 Kinematics of the Proposed XY Motion Stage

The motion of the end-effector is dependent on the active input translational joints and vice versa. The position of the end-effector can be calculated based on the active translational joints (r_1, r_2, r_3 and r_4) based on the following equations:

$$x = r_1 = r_3, \, y = r_2 = r_4$$

4 Fabrication of 4-PP Planar Parallel Robotic Motion Stage

A four-legged 4-PP planar parallel robotic motion stage as depicted in Fig. 1 has been fabricated in-house to perform an experiment to determine the workspace. The experiment is performed to analyse the workspace associated with the manipulator. The fabricated model is depicted in Fig. 2.

The rigid manipulator's base represented by yellow area possesses fixed lengths of 220 mm and 220 mm along X and Y-axes, respectively. The fabricated manipulator is basically a wooden model comprised of NiTi SMA springs as actuators. The passive links used in the model is welding filler rod. The active input translational joints present at each leg move freely in the guide made of electrical wire casing. The available workspace for the end-effector motion is represented by the red box of 160 mm × 160 mm (25,600 mm²) area.

5 Experimental Procedure

The fabricated prototype has been incorporated with nitinol (NiTi), an SMA, in order to actuate the active prismatic joints at each of the legs of the manipulator. The actuator, nitinol, is in the shape of spring with 19 helical windings of which maximum contraction length is ~29 mm under thermal loading. In order to actuate the SMA springs, an electrical current is supplied across it. Due to the resistance of SMA, its temperature rises, thereby leading to thermal loading. Due to a rise in
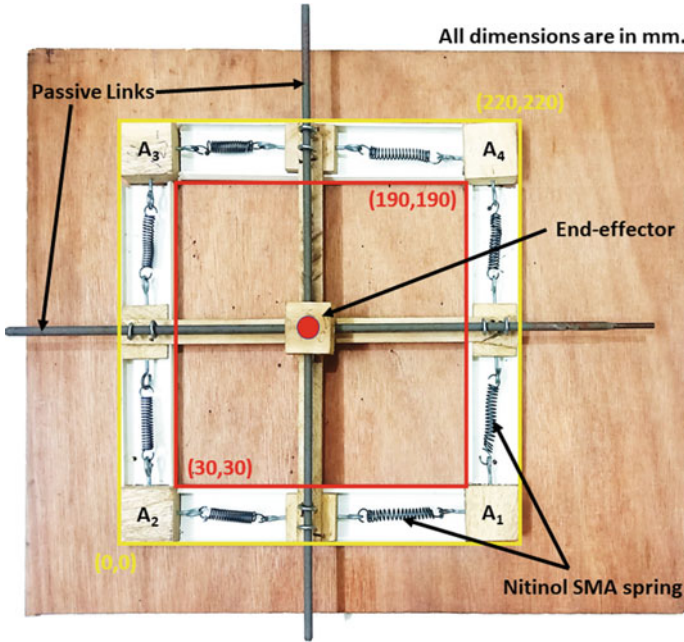
Fig. 2 In-house fabricated model of 4-PP robotic XY motion stage

temperature, the SMA contracts and reaches its maximum contraction length under a certain range of current. The current supplied to the nitinol spring is DC which is supplied with the help of DC power supply (Model: Scientech 4180).

The experimental setup developed for the analysis of 4-PP SMA actuation-based micro-motion stage as depicted in Fig. 3 consists of various devices as specified in Table 1.

The electric current is supplied to only one out of two spring at each leg of the manipulators which leads to its contraction due to thermal load. This leads to the linear motion of the active prismatic joint at the legs of the manipulator. This motion is further transferred with the help of passive joints to the end-effector which reflects in the variation of its position. The new position so obtained is captured as an image in the digital camera (Nikon D5600). Further, AutoCAD is employed to interpret the position of the end-effector in x and y coordinates.

The four active translational or prismatic joints are termed as inputs to the motion stage while rest being passive. The passive joints are dependent on the motion of the active input translation joints. The linear motion at the active prismatic joints with the help of four passive prismatic joints leads to variation in pose (motion along X- and Y-axes) of the end-effector.
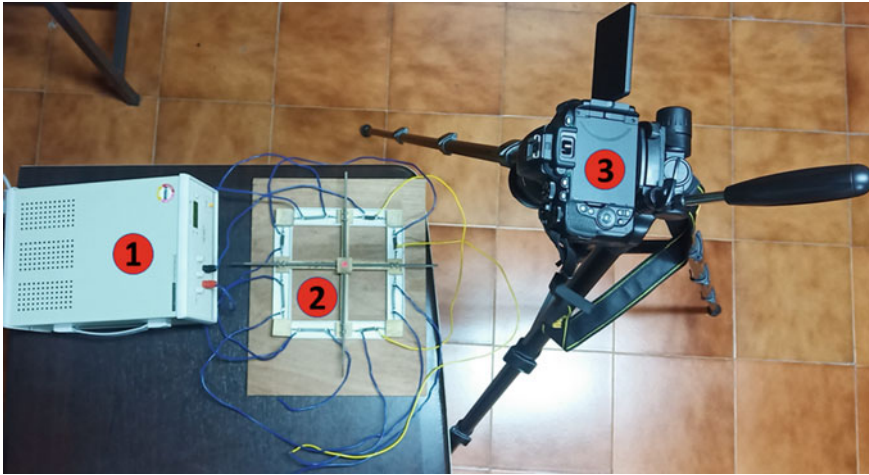
Fig. 3 Experimental setup

Table 1 List of devices for experimental setup

S. No.	Devices	Specifications
1	DC power supply	Scientech 4180 (output: 0–30 V, 0–5 A)
2	Planar parallel manipulator	4-prismatic-prismatic configuration
3	Digital camera with tripod	Nikon D5600

6 Results and Discussion

On application of thermal loading to the SMA springs, the SME occurs which results in a change in shape and size of the SMA to its original form. The spring contracts and its size reduces. The thermal loading is applied by supplying direct electrical current (3–5 A) to the spring which is also known as joule heating. The variation in size of the SMA spring varies the position of the active input translational joints which further affects the end-effector's pose with the help of passive prismatic joints. The forward movement of the active input translational joints in leg 1 and leg 3 together leads to variation in end-effector's pose toward positive X-axis, and its backward movement leads to the motion of the end-effector toward negative X-axis. Similarly, the forward movement of the active input translational joints in leg 2 and leg 4 together leads to variation in end-effector's pose along positive Y-axis, and its backward movement leads to the motion of the end-effector along negative Y-axis.

The pose of the end-effector is kinematically coupled to the active input translation joints (r_1, r_2, r_3 and r_4). Hence, the position of the end-effector is obtained based

Table 2 Four sets of experimental data of the end-effector's pose of the 4-PP motion stage

Direction of the actuation during heating of the SMA springs	Pose of the end-effector (mm)							
	Set-1		Set-2		Set-3		Set-4	
	Q_x	Q_y	Q_x	Q_y	Q_x	Q_y	Q_x	Q_y
Initial position	116.470	114.319	114.470	120.124	117.830	116.046	110.440	114.041
r_1, r_3:F	121.390	116.781	121.510	122.217	124.120	115.661	108.900	115.085
r_1, r_3:B	110.770	115.358	109.280	120.517	107.570	116.170	100.320	115.386
r_2, r_4:F	114.610	124.716	113.590	126.167	115.490	122.773	101.880	120.193
r_2, r_4:B	111.550	108.950	114.720	119.744	115.590	108.874	101.330	110.288
r_1, r_3:F and r_2, r_4:F	122.110	119.949	123.220	126.275	123.170	121.858	107.970	116.913
r_1, r_3:F and r_2, r_4:B	118.580	107.581	122.570	117.827	126.830	111.057	108.600	108.765
r_1, r_3:B and r_2, r_4:F	107.740	119.777	109.330	125.430	105.750	123.870	100.440	119.362
r_1, r_3:B and r_2, r_4:B	113.740	115.476	111.010	115.958	108.450	114.309	100.570	109.539

on various combinations of active prismatic joints and its direction of motion as specified in the first column of Table 2.

Initially, the image of the motion stage is captured and the pose of the end-effector was obtained. Then, the joints r_1 and r_3 were forward actuated which leads to the motion of the end-effector along positive X-axis as discussed previously. After full contraction of the SMA springs (1, 6), an image of the manipulator is captured and the pose of the end-effector was extracted. Furthermore, the backward motion of the same joints r_1 and r_3 were considered which led to the motion of the end-effector along negative X-axis. The pose of the end-effector was obtained for the maximum backward movement of the joints r_1 and r_3. Similarly, the pose of the end-effector was obtained for the forward and backward actuation of the active prismatic joints r_2 and r_4 which led to motion of the end-effector along Y-axis.

Till now, the motion of the end-effector was along a single axis. Now, the active prismatic joints r_1, r_2, r_3 and r_4 were actuated in the combination of forward and backward movements which led to the motion of the end-effector along both X and Y-axes simultaneously. The image was captured, and the end-effector pose was extracted for each condition as specified in Table 2.

(a) Set-2 - r$_1$, r$_3$:F and r$_2$, r$_4$:F   (b) Set-2 - r $_1$, r$_3$:F and r$_2$, r$_4$:B   (c) Set-2 - r $_1$, r$_3$:B and r$_2$, r$_4$:F
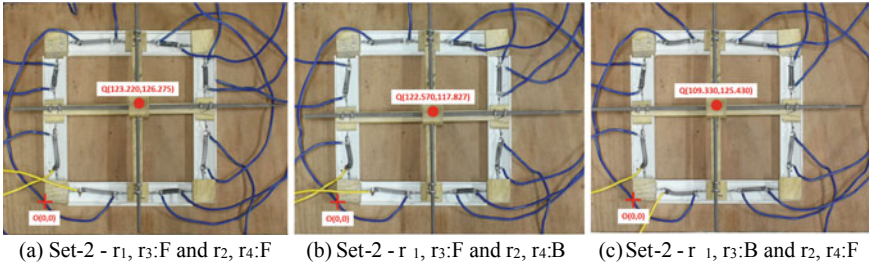
Fig. 4 End-effector pose of the proposed *XY* micro-motion stage

Four sets of experiments were conducted on the in-house fabricated 4-PP planar parallel micro-motion stage, and the obtained data are presented in Table 2 of which few experimental images are depicted in Fig. 4.

where *F* and *B* represent forward and backward actuation of the SMA springs, respectively.

The experiment showed gradual variation in the pose of the end-effector with gradual variation in the position of the active input translational joints. From the experimental data in Table 2, the minimum and maximum position of the end-effector along both *X* and *Y*-axes obtained are specified in Table 3. The range of deflection along both the axes denotes the stroke length of 26.51 mm and 18.694 mm along *X* and *Y*-axes, respectively. Hence, the total experimental workspace area is 495.578 mm^2 as depicted in Fig. 5.

Although the available workspace area is 160 mm × 160 mm, the presence of – (i) certain width of active prismatic joints, (ii) presence of hooks to which springs are connected and (iii) maximum possible contraction of spring is 29 mm – minimizes the workspace area. Hence, the workspace area in which the end-effector is feasible to undergo motion is 34 mm × 34 mm (i.e. 1156 mm^2) and is represented as feasible workspace in Fig. 5.

Figure 5 clearly depicts the variation in workspace regions of feasible workspace and experimental workspace which is an indication of the presence of certain inefficiency. The percentage of loss in the workspace is given as

$$\text{Percentage loss} = (\text{Feasible Workspace} - \text{Experimental Workspace})$$
$$100/\text{Feasible Workspace} = (1156 - 495.578)100/1156$$
$$= 57.13\%$$

Table 3 Stroke length of the end-effector along the coordinate axes

Direction	Deflection of the end-effector		Stroke length (mm)
	Minimum (mm)	Maximum (mm)	
X-axis	100.320	126.830	26.510
Y-axis	107.581	126.275	18.694

Fig. 5 Workspace of 4-PP
robotic micro-motion *XY*
stage
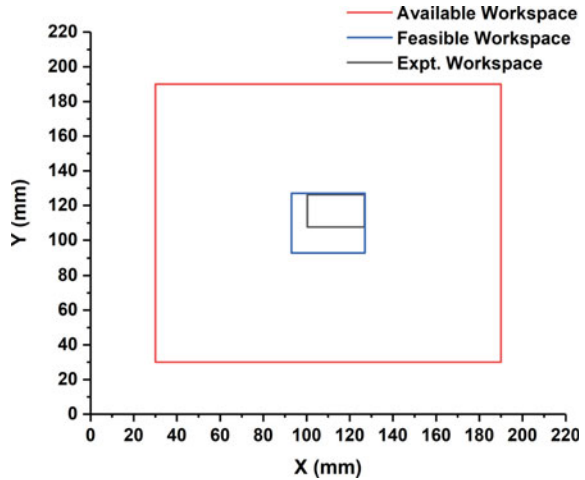
Hence, the efficiency associated with the in-house fabricated model is 42.87%.

7   Conclusion

The major conclusions associated with this study have been outlined below:

1. A 4-PP planar parallel robotic micro-motion stage was fabricated.
2. The feasible and experimental workspace associated with the in-house fabricated model is 1156 mm^2 and 495.578 mm^2, respectively.
3. The experimental workspace of the in-house fabricated model showed an efficiency of 42.87%.

References

1. K. Otsuka, C. Wayman, Shape memory material. Cambridge University Press, Cambridge. ISBN: 9780521663847 (1998)
2. F. Ronnie, O. Ozkan, H. Robert, R. Shalom, T. Tsu-Chin, P. James, L. Tiffany, B. John, C. Greg, Multi-scale alignment and positioning system–MAPS. Prec Eng **36**(4), 517–537 (2012)
3. Y. Shimizu, P. Yuxin, K. Junji, A. Toyohiro, I. So, G. Wei, L. Tien-Fu, Design and construction of the motion mechanism of an XY micro-stage for precision positioning. Sens. Actuators A **201**, 395–406 (2013)
4. J. Lee, D.W. Lee, Fabrication of a micro XY-stage using SU-8 thermal actuators. Microelectron. Eng. **86**(4), 1267–1270 (2009)
5. Y. Qin, B. Shirinzadeh, Y. Tian, D. Zhang, Design issues in a decoupled XY stage: static and dynamics modelling, hysteresis compensation, and tracking control. Sens. Actuators A **194**, 95–105 (2013)

6. Y. Qing, J. Dong, P.M. Ferreira, Design, analysis, fabrication and testing of a parallel-kinematic micropositioning XY stage. Int. J. Mach. Tools Manuf. **47**(6), 946–961 (2007)
7. P. Wang, Q. Xu, Design of a flexure-based constant-force XY precision positioning stage. Mech. Mach. Theor. **108**, 1–13 (2017)
8. Y.J. Choi, S.V. Sreenivasan, B.J. Choi, Kinematic design of large displacement precision XY positioning stage by using cross strip flexure joints and over-constrained mechanism. Mech. Mach. Theor. **43**(6), 724–737 (2008)
9. Y. Singh, S. Mohan, Development of a planar 3PRP parallel manipulator using shape memory alloy spring based actuators. In *Proceedings of the Advances in Robotics*, ACM, 10 (2010)
10. C. Jun, Qin, M.P. Sun, Y. Qin, A prototype micro-wheeled-robot using SMA actuator. Sens. Actuators A Phys. **113**(1), 94–99 (2004)
11. B. Kim, M.G. Lee, Y.P. Lee, Y. Kim, G. Lee, An earthworm-like micro robot using shape memory alloy actuator. Sens. Actuators A **125**(2), 429–437 (2006)
12. M.J. Jaronie, L. Martin, S. Aleksandar, A.G. Mark, A review of shape memory alloy research, applications and opportunities. Mater. Des. **56**, 1078–1113 (2014)